Intertemporal Uncertainty Management in Gas-Electric Energy Systems using Stochastic Finite Volumes

Saif R. Kazi*, Kaarthik Sundar†, Sidhant Misra*, Svetlana Tokareva* and Anatoly Zlotnik*
*Applied Mathematics and Plasma Physics Group, Los Alamos National Laboratory
†Information Systems and Modeling Group, Los Alamos National Laboratory

***Abstract*—The reliance of power systems on gas-fired generators that run on timely delivery of natural gas compels new methods for coordinating electricity markets and gas pipeline operations. Concurrently, the growth in power generation by intermittent and uncontrollable renewable energy sources increases uncertainty in spatiotemporal electricity loads that propagates to interconnected pipeline systems. This has been addressed by day-ahead uncertainty management frameworks, including a joint optimization problem with chance constraints for optimal power flow and robust optimization to handle interval uncertainty in pipeline scheduling. While that formulation is tractable and ensures feasibility of the integrated system with high probability, it results in highly conservative pipeline flow scheduling. We propose a two-stage formulation where a stochastic finite volume representation for nonlinear gas flow with uncertain boundary conditions is used to manage intertemporal uncertainties for a pipeline that supplies fuel to peaking plants that provide operating reserves to an electricity market. This allows calibration of power production and reserves together with pipeline flow schedules with probabilistic guarantees using chance constraints for both networks. We describe chance-constrained formulations for power and gas networks and demonstrate the workflow using 3-bus, 1-pipe and 24-bus, 24-pipe gas-electric network cases.**

***Index Terms*—gas-electric coordination; operations; uncertainty quantification; DC power flow; gas pipelines**

I. Introduction

Roughly 25% of worldwide electricity generation is fueled by natural gas, which is viewed as playing a major role in the transition to net-zero energy systems [1]. Natural gas-fired generators emit far less carbon dioxide and other pollutants than coal power plants and are much easier to site, permit, and build than nuclear generation stations [2]. In addition to combined-cycle plants that provide base load, gas-fired peaking plants can quickly ramp up output to compensate for shortfalls in production by variable and intermittent renewable sources. This has resulted in a reliance of the power grid on gas-fired generation that is fueled by just-in-time delivery of natural gas through pipeline systems, whose managers are challenged to respond to changes in fuel loads on the faster time-lines of power system decision making [3]. Significant attention has been paid to the interdependence between power grids and natural gas pipeline networks, and managing uncertainty in generation timing that arises from demand and uncontrollable renewable wind and solar remains compelling.

Prior studies on joint gas-electric grid optimization for day-ahead planning have modeled the physics of energy flow in the power grid using the direct current (DC) model typically used in the unit commitment (UC) problem, and approximate the nonlinear gas flow equations to model pipeline network response to variable hourly consumption by gas-fired generators [4]. A standard approach to uncertainty management for this problem is to use stochastic optimization, which results in well-known issues of challenging computational scaling arising due to sampling of parameters in the uncertainty region [5], [6]. A popular method of representing the stochastic optimization problem for optimal power flow (OPF) given uncertain loads involves so-called chance constraints, which place a limit on the probability that an inequality constraint is violated [7]. Under assumption of Gaussian uncertainty and linear or linearlized models of power flow, chance-constrained OPF problems can be solved efficiently [8]. This technique has been incorporated in recent studies aiming to represent the joint gas-electric stochastic optimization problem using deterministic approximations, where Gaussian uncertainty is managed for the power grid using chance constraints and interval uncertainty is managed for the pipeline system by using robust optimization with extremal scenario constraints [9]. Feasibility guarantees for interval uncertainty are provided by invoking the monotonicity property, which guarantees that ordered boundary conditions of gas flows throughout a pipeline network correspond to ordered pressures, and this is shown to hold in the usual physical regime of gas pipeline operations carrying roughly homogeneous gas [10]. A strictly increasing linear or quadratic heat rate curve is typically assumed for joint gas-electric network formulations.

While the approach of chance-constrained power flow together with robust interval gas pipeline constraints results in a tractable formulation and yields feasible solutions, the operating set-points it provides are typically too conservative in requiring excessive pressurization of pipelines in case the line-pack is needed to fuel a peaking plant [9]. Such a solution essentially guarantees that the pipeline network is sufficiently pressurized to provide reserves at each hour when they are scheduled, but not necessarily dispatched. Because the likelihood that reserve activation is required to fulfil a

Submitted to the 23rd Power Systems Computation Conference (PSCC 2024).

potential power system load scenario may be low, the solution provides too much margin in the form of reserve line-pack, and this prevents the full capacity of the pipeline network from being used to provide ramping flexibility. A method to apply chance constraints to the inequalities in gas pipeline intra-day dynamic optimization would provide less conservative solutions, but this has been elusive. Uncertainty quantification (UQ) for gas pipeline flows is notoriously complex, because of the significant nonlinearity and computational complexity involved [11]. The challenge has to an extent been met by a new stochastic finite volume (SFV) method for UQ in gas pipeline flows, which was recently shown to model the propagation of uncertainty in initial boundary value problems (IBVPs) for gas flow in pipeline networks [12].

In this paper, we use the SFV representation for solutions of the nonlinear gas flow equations with uncertain boundary conditions to manage *intertemporal* uncertainties for a pipeline system. Intertemporal uncertainty in this context is used to denote a temporary increase in load starting at a time that is randomly distributed (e.g. uniformly on an interval). We propose this type of uncertainty modeling to represent the likely activation of a peaking plant for a brief time interval (e.g., 2 hours) but at an *a priori* unknown time in a part of the day-ahead planning interval, which reasonably represents the uncertainty that gas pipeline operators experience due to lack of visibility into power grid operations. The primary contribution of our study is a chance-constrained model-predictive optimal scheduling and reserve allocation problem for integrated gas-electric systems. In conjunction with the proven method of chance-constraints, our joint uncertainty management scheme provides probabilistic robustness guarantees by computing a minimum value for the extra reserve requirements for both the power and gas delivery networks.

The remainder of this paper is as follows. We first describe a multi-period stochastic optimal power flow formulation in Section II, and then describe a chance-constrained dynamic optimal gas flow formulation that accounts for intertemporal load uncertainty in Section III. We then describe the computational implementation and limited computational studies in Section IV, and conclude in Section V.

II. Multi-period Stochastic DC-OPF

We employ a simple continuous-time approximation of the multi-period DC OPF problem, which is similar to that used in a previous study [3], and extend it to a stochastic formulation with probabilistic constraints. Further, we approximate this formulation in a discretized stochastic space using integer variables, so that the chance-constrained OPF can be stated as a mixed-integer linear program. We suppose that the power system is represented by a set of nodes N_p connected by lines E, with generators G and loads $\mathsf{N_d}$.

A. Deterministic Multi-period DC-OPF

Consider a continuous-time formulation of a day-ahead power system economic dispatch problem, in which the minimized objective is the total running marginal cost of electricity production over the planning period:

$$\min \sum_{g\in\mathsf{G}} \int_{t=0}^{t=T_f} f(P_g(t))dt \tag{1a}$$

$$\text{s.t.} \sum_{i\in\partial^+ j} P_{ij}(t) - \sum_{k\in\partial^- j} P_{jk}(t) = P_g(t) - P_d(t), \quad \forall j \in \mathsf{N_p}, \forall t, \tag{1b}$$

$$b_{ij}(\theta_i(t) - \theta_j(t)) = P_{ij}(t) \qquad \forall (i,j) \in \mathsf{E}, \forall t, \tag{1c}$$

$$P_{ij}^{min}(t) \le P_{ij}(t) \le P_{ij}^{max}(t) \qquad \forall (i,j) \in \mathsf{E}, \forall t, \tag{1d}$$

$$P_g^{min}(t) \le P_g(t) \le P_g^{max}(t) \qquad \forall g \in \mathsf{G}, \forall t. \tag{1e}$$

The constraints (1b)-(1c) represent the DC power flow equations, and (1d)-(1e) represent the line flow limits and generator production limits evaluated point-wise in time. We denote the marginal production cost function by $f(\cdot)$, the production of generator $g \in \mathsf{G}$ by $P_g(t)$, the consumption by a load $d \in \mathsf{N_d}$ as $P_d(t)$, the power flow on line $(i,j) \in \mathsf{E}$ by $P_{ij}(t)$, and the voltage phase angle at bus $j \in \mathsf{N}$ by θ_j. The parameters b_{ij} are line impedance values. The continuous-time formulation in equations (1a) can be expressed in discrete time on the set of time points $\{0, \Delta t, 2\Delta t, ..., T_f\}$ with intervals Δt:

$$\min \sum_{g\in\mathsf{G}} \sum_{t=0}^{t=T_f} f(P_g^t) \tag{2a}$$

$$s.t. \sum_{i\in\partial^+ j} P_{ij}^t - \sum_{k\in\partial^- j} P_{jk}^t = P_g^t - P_d^t \quad \forall j \in \mathsf{N_p}, \forall t, \tag{2b}$$

$$b_{ij}(\theta_i^t - \theta_j^t) = P_{ij}^t \qquad \forall (i,j) \in \mathsf{E}, \forall t, \tag{2c}$$

$$P_{ij}^{min} \le P_{ij}^t \le P_{ij}^{max} \qquad \forall (i,j) \in \mathsf{E}, \forall t, \tag{2d}$$

$$P_g^{min} \le P_g^t \le P_g^{max} \quad \forall g \in \mathsf{G}, \forall t. \tag{2e}$$

The formulation (2) can be directly implemented using a linear or nonlinear programming solver, based on the form of $f(\cdot)$.

B. Stochastic Discretized Multi-period DC-OPF

Our goal is to develop a joint electricity and gas network day-ahead planning formulation that accounts for intertemporal uncertainty, so system operators are prepared to serve additional load that occurs at an unknown time. We develop a streamlined model where uncertainty management is the key modeling aspect of interest, supposing that common modeling aspects such as commitment variables, ramping constraints, AC power flow, and other elements of power system day-ahead planning could be added in practice. We thus define an *uncertain inter-temporal power load* P_d^t, of form

$$P_d^t = \bar{P}_d^t + \tilde{P}_{s,d}^t, \qquad \forall s \in \mathsf{S}, t \in \mathsf{T}, d \in \mathsf{N_d}, \tag{3}$$

where $\bar{P}_d^t$ is a baseline load and $\tilde{P}_{s,d}^t$ are a collection of additional load contingency scenarios indexed by the scenario set S, such that $\sum_{s\in\mathsf{S}} \mathbb{P}(s) = 1$. We suppose that the uncertain excess power scenarios $\tilde{P}_{s,d}^t$ take the form of a re-scaled trapezoidal function H, as illustrated in Figure 1, with steep ramp-up to and ramp-down from an amplitude h_s, of form

$$\tilde{P}_{s,d}^t = h_s H(t - t_s). \tag{4}$$

The initial time t_s of the additional load $\tilde{P}^t_{s,d}$ is random and depends on the scenario s in set of uncertain scenarios S.

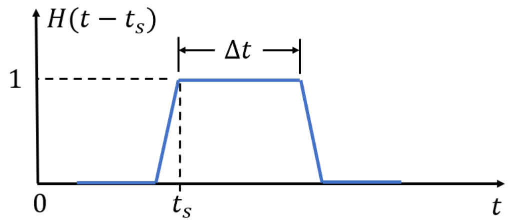

Fig. 1. Trapezoidal load scenario of duration Δt starting at time t_s.

To modify the OPF formulation (2) to include reserve generation with probabilistic guarantees, we define the reserve power variable R^t_r and reserve participation factor as α_r, where each $r \in \mathsf{R} \subseteq \mathsf{G}$ corresponds to a generator that participates in reserve provision. The constraint (2e) is modified to bound the total scheduled production and scheduled reserves for each of these generators within its production limits according to

$$P_g^{min} \leq P^t_g + R^t_r \leq P^{max}_g \quad \forall r \in \mathsf{R} \subseteq \mathsf{G}, g \in \mathsf{G}. \tag{5}$$

We consider a linear objective that approximates marginal costs of generating power and allocating reserve power as

$$f(P^t_g, R^t_r) = \sum_{g \in G} c_g P^t_g + \sum_{r \in R} c_r R^t_r. \tag{6}$$

Finally, rather than enforce strict feasibility limits on the multi-period OPF problem, we determine production and reserve schedules that allow for a small chance that the reserve requirements may not be met. Such chance-constrained OPF strategies have shown significant improvement in objectives at the cost of only a small chance of constraint violations [7], [13]. We apply probabilistic chance constraint for the power flow problem of form

$$\mathbb{P}\left(\alpha_r \sum_{d \in \mathsf{N_d}} \tilde{P}^t_{s,d} - R^t_r \leq 0\right) \geq 1 - \epsilon_p, \quad \forall t \in \mathsf{T}, r \in \mathsf{R}, \tag{7}$$

in total probability, where no assumption is made on the scenario $s \in \mathsf{S}$. Here α_r are the *reserve participation factors* for generators, which sum to unity:

$$\sum_{r \in \mathsf{R}} \alpha_r = 1. \tag{8}$$

The inequality (7) can be written in terms of marginal and conditional probabilities as

$$\sum_s \mathbb{1}\left(\alpha_r \sum_{d \in \mathsf{N_d}} \tilde{P}^t_{s,d} - R^t_r \leq 0\right) \nu(s) \geq 1 - \epsilon_p, \quad \forall t \in \mathsf{T}, r \in \mathsf{R}, \tag{9}$$

where ν is a measure on the stochastic scenarios, i.e., the marginal probability $\nu(s) = \mathbb{P}(s)$. The conditional probability in the inequality (9) can be written as an indicator function, because the chance constraint for scenario $s \in \mathsf{S}$ is enforced only if the scenario occurs. Using constraints (5), (8), and (9) in place of constraint (2e), and the objective (6) in place of equation (2a), results in a formulation where reserves are allocated with a guarantee that the independent contingency scenarios S can be served with total probability $1 - \epsilon_p$.

C. Integer-based Formulation

Formulating the conditional probabilities using indicator functions in equation (9) results in a non-smooth and non-convex optimization problem. We reformulate this using binary integer variables to build a mixed integer programming (MIP) problem. Define a set of binary variables $z^{s,t}_r \in \{0, 1\}$ $\forall s \in \mathsf{S}$, $t \in \mathsf{T}$ corresponding to the indicator functions as

$$\begin{cases} z^{s,t}_r = 1 \longleftrightarrow \left(\alpha_r \sum_{d \in N_d} \tilde{P}^t_{s,d} - R^t_r \leq 0\right), \\ z^{s,t}_r = 0 \longleftrightarrow \left(\alpha_r \sum_{d \in N_d} \tilde{P}^t_{s,d} - R^t_r \geq 0\right). \end{cases} \tag{10}$$

The chance constraint can then be stated as

$$\sum_{s=1}^{N_s} z^{s,t}_r \nu(s) \geq 1 - \epsilon_p. \tag{11}$$

We then apply the big-M reformulation to rewrite the disjunctive constraints, for $\forall s \in \mathsf{S}$, $t \in \mathsf{T}$, and $r \in \mathsf{R}$, as

$$X^{s,t}_g = \alpha_r \sum_{d \in N_d} \tilde{P}^t_{s,d} - R^t_r, \tag{12a}$$

$$-P^{max}_g z^{s,t}_r \leq X^{s,t}_r \leq (1 - z^{s,t}_r) \sum_{d \in N_d} \tilde{P}^t_{s,d}. \tag{12b}$$

The result is a mixed-integer linear program (MILP) for chance-constrained OPF of form

$$\begin{aligned} \min \quad & \text{Objective Eq. (6)} \\ \text{s.t.} \quad & \text{DC Power Flow Eq. (2b)-(2c)} \\ & \text{Line Flow Limits Eq. (2d)} \\ & \text{Generator Production Limits Eq. (5)} \\ & \text{Participation Factors Eq. (8)} \\ & \text{Chance Constrained Reserve Adequacy Eq. (11)} \\ & \text{Disjunctive Conditional Binary Values Eq. (12)} \end{aligned} \tag{13}$$

III. Intertemporal Uncertainty Management for a Gas Pipeline Network

We develop a formulation for managing intertemporal uncertainty in gas pipeline flow scheduling in order to enable more effective support of power systems through gas-fired generation. The approach is an extension of a now standard deterministic formulation for dynamic optimal gas flow [14], which we review below.

A. Dynamic Optimal Gas Flow

We start with the fundamental partial differential equations (PDEs) for gas transport in a pipe [15],

$$\frac{\partial \rho}{\partial t} + \frac{\partial \phi}{\partial x} = 0, \tag{14a}$$

$$\frac{\partial \phi}{\phi t} + \frac{\partial (p + \frac{1}{2}\rho u^2)}{\partial x} = -\frac{\lambda}{2D}\frac{\phi|\phi|}{\rho}, \tag{14b}$$

with initial conditions $\rho(0, x) = \rho_0(x)$, $\phi(0, x) = \phi_0(x)$ and boundary conditions $\rho(t, 0) = \rho_s(t)$, $\phi(t, L) = \phi_L(t)$. Here

ρ, p, ϕ, and u are gas density, pressure, per area mass flux, and velocity, respectively, and λ and D are the friction factor and pipe diameter. We apply the typical simplifying assumptions [16] that the ideal gas equation of state $p = a^2\rho$ can be used (where a is the wave speed in the gas), that transients are slow so that $\rho u^2 << p$, and friction dominates the flux derivative term $\partial\phi/\partial t$ so that the latter can be neglected. Following established approaches [17], [18], we discretize the equations (14a) using a lumped-element approximation. Integrating Eq. (14a) over a pipe segment of length L yields

$$L\frac{d\rho^+(t)}{dt} + 2\phi^-(t) = 0, \tag{14c}$$

$$a^2\rho^-(t) = -\frac{\lambda L}{4D}\frac{\phi^+(t)|\phi^+(t)|}{\rho^+(t)}, \tag{14d}$$

$$\rho^+(0) + \rho^-(0) = \rho_0(L), \tag{14e}$$

where we denote

$$\rho^+(t) = \frac{\rho(t,L)+\rho(t,0)}{2},\ \rho^-(t) = \frac{\rho(t,L)-\rho(t,0)}{2}, \tag{15}$$

$$\phi^+(t) = \frac{\phi(t,L)+\phi(t,0)}{2},\ \phi^-(t)= \frac{\phi(t,L)-\phi(t,0)}{2}. \tag{16}$$

We suppose that a pipeline network can be defined on a graph where $\mathcal{N}$ is the set of nodes (junctions) and $\mathcal{E} = \mathcal{P}\cup\mathcal{C}$ is a set of edges connecting pairs of nodes, where $\mathcal{P}$ and $\mathcal{C}$ are sets of pipes and compressors. We denote correspondences between edge boundary variables and nodal variables as

$$\rho_{ij}(0,t) = \rho_i(t),\ \ \rho_{ij}(L_{ij},t) = \rho_j(t), \tag{17a}$$

$$\phi_{ij}(0,t) = \phi_{ij}^{in}(t) = \phi^+(t) - \phi^-(t), \tag{17b}$$

$$\phi_{ij}(L,t) = \phi_{ij}^{out}(t) = \phi^+(t) + \phi^-(t). \tag{17c}$$

The above notations enable us to state a reduced network optimization model for the dynamic optimal gas flow (DOGF) problem [19], [14] as follows:

$$\min \sum_{c\in C}\int_{t=0}^{t=T_f} \phi_c(t)(\mu_c(t)-1)dt \tag{18a}$$

$$\text{s.t. } L_{ij}(\dot{\rho}_{ij}^+(t)) + 4\phi_{ij}^-(t) = 0,\ \forall(i,j)\in\mathcal{P}, \tag{18b}$$

$$\rho_j^2(t)-\rho_i^2(t) = -\frac{\lambda_{ij}L_{ij}}{a^2D_{ij}}\phi_{ij}^+(t)|\phi_{ij}^+(t)|,\ \forall(i,j)\in\mathcal{P}, \tag{18c}$$

$$\sum_{i\in\partial^+j}\phi_{ij}^{out}(t)A_{ij} - \sum_{k\in\partial^-j}\phi_{jk}^{in}(t)A_{jk} = q_j(t),\ \forall j\in\mathcal{N}, \tag{18d}$$

$$\rho_j(t) = \mu_{ij}(t)\rho_i(t),\ \forall(i,j)\in\mathcal{C}, \tag{18e}$$

$$p^{\min} \le a^2\rho_i(t) \le p^{\max},\ \forall i\in\mathcal{N}, \tag{18f}$$

$$\rho_i(0) = \rho_i(T_f), \forall i\in\mathcal{N}. \tag{18g}$$

In the above formulation, the objective $\phi_c(t)(\mu(t)-1)$ in Eq. (18a) is a bilinear proxy for the adiabatic work done by a compressor $c\in\mathcal{C}$ where $\mu_c = \mu_{ij}$ is the compressor ratio acting as in Eq. (18e) and $\phi_c(t)$ is the through-flow. The constraint (18d) represents nodal mass flow balance, where A_{ij} is the cross-section area of pipe (i,j) and $q_j(t)$ is the mass flow withdrawn from node $j\in\mathcal{N}$. The indexing sets ∂^+j and ∂^-j are sets of nodes connected to pipes incoming to and outgoing from node j, respectively. The constraint (18f) requires system pressures to stay within minimum and maximum bounds, which we assume to be uniform network-wide. The constraint (18g) enforces C^1 time-periodicity for nodal densities (and thus pressures and all other decision functions), which is crucial to well-posedness of the optimal control problem (OCP) and well-behaved solutions.

B. Chance-Constrained Intertemporal Uncertainty

Recall that we define by *intertemporal uncertainty* a temporary increase in load starting at a time that is unknown and randomly distributed (e.g. uniformly on an interval), and propose this as a model for the likely activation of a gas-fired peaking plant, which reasonably represents the uncertainty that gas pipeline operators experience due to lack of visibility into power grid operations. The key concern in coordination of power systems, gas-fired generation, and gas pipelines is ensuring electricity production while maintaining adequate pipeline pressures. The lower bound in constraint (18f) is somewhat flexible, as long as it is not violated significantly or for long periods. We therefore enforce this limit using chance constraints, allowing for a small chance of violation during a short period of uncertain timing.

Suppose that a subset of gas pipeline nodes $j\in\mathcal{S}\subset\mathcal{N}$ has stochastic gas consumption profiles of the form

$$q_j(t,\omega) = \bar{q}_j(t) + \tilde{q}_jH(t-t_\omega), \tag{19}$$

where $t\in\mathsf{T} := [0,T_f]$ and $t_\omega\in\mathsf{T}_\Omega\subset\mathsf{T}$. In a typical setting, $T_f = 24$ hours and $\mathsf{T}_\Omega = [6,18]$ hours. We may suppose that $q_j(t,\omega) = \bar{q}_j(t)$ for $j\in\mathcal{N}\setminus\mathcal{S}$. The functions $\bar{q}_j(t)$ and $\tilde{q}_j(t)$ denote the nominal baseline load at a node and the quantity of the uncertain load, if it occurs at time t. Here H denotes the same type of temporary increase in load of duration Δt (typically $\Delta t = 1$ hour) as illustrated in Figure 1. The uncertainty is in the timing t_ω of augmented load, where for simplicity we suppose that $t_\omega\in T_\Omega$ is distributed uniformly, although other distributions may be used. This represents the point of view of a gas pipeline manager, who sees a peaking gas-fired generator as likely to operate for a short period at some point during a congested time of the day, but with uncertain timing. To express the chance constraint for pipeline pressure, we define a quadratic penalty function

$$\Gamma(z) = \begin{cases}\gamma z^2, & \text{if } x\ge 0,\\ 0, & \text{otherwise,}\end{cases} \tag{20a}$$

and define a penalized minimum pressure violation variable

$$v_j^{min}(t,\omega) = \Gamma\left(\frac{p^{min}}{a^2} - \rho_j(t,\omega)\right). \tag{20b}$$

The quadratic penalty is chosen in order to reflect that larger violations of the lower pressure limits are more problematic. Additionally, because it is twice differentiable, it facilitates a well-behaved nonlinear program. The chance constraint is then expressed as

$$\mathbb{E}_\omega\left[v_j^{min}(t,\omega)\right] \le \epsilon_g, \qquad \forall t\in T. \tag{21}$$

In order to approximate constraint (21) in a deterministic manner (i.e., without requiring Monte Carlo simulation), we apply the SFV method as follows. We discretize the stochastic space Ω, which has one-to-one correspondence with the interval T_Ω on which the random time t_ω appears, into M cells delimited by $M+1$ boundary points, each of which corresponds to a value of t_ω. We construct the penalty function variable using a third order spline expansion on Ω as

$$v_j^{min}(t,\omega) = \sum_{m \in M} a_{jm}(t) b_{jm}(\omega), \tag{22a}$$

where $b_{jm}(\omega)$ is the m-th spline function on the stochastic space grid that is completely known. The constraint (21) can then be expressed as an expectation over ω as

$$\sum_{m \in M} a_{jm}(t) \int_\omega b_{jm}(\omega) d\omega \le \epsilon_g, \qquad \forall t \in T, \tag{22b}$$

where the coefficients $a_{jm}(t)$ are decision functions that can be optimized. The presence of stochastic parameters leads to state variables that are also stochastic, and the optimization task is to choose deterministic planning profiles for gas compressors $\mu_c(t)$ for $c \in \mathcal{C}$ such that state variables satisfy all constraints. The objective function must also be evaluated in expectation. The chance-constrained dynamic optimal gas flow for intertemporal uncertainty management is formulated as

$$\min \sum_{c \in C} \int_{t=0}^{t=T_f} \mathbb{E}_\omega \phi_c(t,\omega)(\mu_c(t)-1) dt. \tag{23a}$$

$$\text{s.t. } L_{ij}(\dot{\rho}_{ij}^{+}(t,\omega)) + 4\phi_{ij}^{-}(t,\omega) = 0, \quad \forall (i,j) \in \mathcal{P},\ \forall \omega \in \Omega \tag{23b}$$

$$\rho_j^2(t,\omega) - \rho_i^2(t,\omega) = -\frac{\lambda_{ij} L_{ij}}{a^2 D_{ij}} \phi_{ij}^{+}(t,\omega)|\phi_{ij}^{+}(t,\omega)|, \quad \forall (i,j) \in \mathcal{P}, \forall \omega \in \Omega \tag{23c}$$

$$\sum_{i \in \partial^+ j} \phi_{ij}^{out}(t,\omega) A_{ij} - \sum_{k \in \partial^- j} \phi_{jk}^{in}(t,\omega) A_{jk} = q_j(t,\omega), \quad \forall j \in \mathcal{N},\ \forall \omega \in \Omega \tag{23d}$$

$$\rho_j(t,\omega) = \mu_{ij}(t)\rho_i(t,\omega),\ \forall (i,j) \in \mathcal{C}, \forall \omega \in \Omega \tag{23e}$$

$$a^2 \rho_i(t,\omega) \le p^{\max},\ \forall i \in \mathcal{N}, \forall \omega \in \Omega \tag{23f}$$

$$v_j^{min}(t,\omega) = \Gamma_{pen}\left(\frac{p^{min}}{a^2} - \rho_j(t,\omega)\right), \quad \forall j \in \mathcal{S},\ \forall \omega \in \Omega, \tag{23g}$$

$$v_j^{min}(t,\omega) = \sum_{m \in M} a_{jm}(t) b_{jm}(\omega), \forall j \in \mathcal{S},\ \forall \omega \in \Omega, \tag{23h}$$

$$\sum_{m \in M} a_{jm}(t) \int_\omega b_{jm}(\omega) d\omega \le \epsilon_g, \forall j \in \mathcal{S}, \tag{23i}$$

$$\rho_i(0,\omega) = \rho_i(T_f,\omega),\ \forall i \in \mathcal{N},\ \forall \omega \in \Omega. \tag{23j}$$

C. Time Discretization

We discretize problem (23) in time on $\mathsf{T} = [0, T^f]$ using N points $\{t_n\}_{n=1}^N$ defined by $t_n = \Delta t \cdot (n-1)$ for $n = 1, 2, \ldots, N$. The time derivatives $\dot{\rho}_j(t_n)$ are approximated using a simple first order forward finite difference formula as

$$\dot{\rho}_{ij}^{+}(t_n,\omega) \approx \frac{1}{\Delta t}(\rho^{+}(t_{n+1},\omega) - \rho^{+}(t_n,\omega)), \tag{24}$$

where ρ^+ is as defined in (15). To represent the cyclic boundary conditions on the state variables in (23j), we use

$$\dot{\rho}_{ij}^{+}(t_N) \approx \frac{1}{\Delta t}(\rho^{+}(0,\omega) - \rho^{+}(t_{N-1},\omega)), \tag{25}$$

which implicitly includes the cyclic condition (23j) and thus reduces the number of variables and constraints. This leads to a computationally well-posed OCP that, when discretized, results in a nonlineer program (NLP) with good numerical conditioning and well-behaved solutions, both conceptually and computationally. The application of gas-electric system coordination using deterministic models with cyclic boundary conditions applied in a rolling-horizon manner to non-periodic boundary data was demonstrated previously [20].

IV. Computational Studies

We evaluate power and gas network uncertainty management using a workflow that consists of two sequential optimization solves. Given a power grid model with nominal parameters and a set of stochastic scenarios, we solve the MILP formulation (13) to obtain a power flow solution that includes production schedules P_g^t for each generator $g \in \mathsf{G}$ as well as reserve allocation R_g^t for generators that participate. Using idealized generator-dependent linear heat rate functions $h_g(x) = R_h x$, we transform these to get baseline and uncertain gas demand curves as $\bar{q}_j(t) = h_g(P_g^t)$ and $\tilde{q}_j(t) = h_g(R_g^t)$. The stochastic intertemporal gas consumption model for generator g is as defined in Eq. (19), and is used in Eq. (23d) when solving problem (23). We use $\epsilon_p = \epsilon_g \equiv 0.1$ as violation probabilities for power and gas chance constraints.

The stochastic power problem (13) is solved with the MILP solver HiGHS [21] in the Julia based modeling language JuMP [22], whereas the stochastic dynamic optimal gas flow problem (23) is solved using the NLP solver KNITRO [23]. The problems are solved for a 24-hour time horizon with $T_f = 24$ hours. Because the problem is non-convex, there are no global optimality guarantees for the NLP solver solution, but a *feasible* solution is ensured for a local optimum.

TABLE I
Power Network Size Parameters

N_b	# of buses	3	24
N_k	# of reference buses	1	1
N_l	# of power lines	3	38
N_d	# of loads	3	17
N_g	# of total generators	3	33
N_r	# of gas reserve generators	1	18
N_t	# of time points	25	25
N_s	# of scenarios	50	50

We consider a case study with a 3-bus power system and single pipe, as illustrated in Figure 2, and another case study with the IEEE RTS-96 24-node power test system coupled to a 24-pipe gas pipeline test network, which is described in detail in previous studies [3], [9]. For the power system formulation

(13), the optimization problem sizes for the studies are shown in Table I. The power flow formulation has $(N_r + N_b + N_l + N_g) \times N_t + N_r$ continuous and $N_r \times N_t \times N_s$ binary variables, $(N_b + N_l + N_k) \times N_t$ equality constraints, and $2 \times N_r \times n_t + N_r \times N_t \times N_s$ inequality constraints. This results in 1501 variables (1250 binary + 251 continuous) and 1551 constraints (151 equality + 1350 inequality) for the 3-bus system, and 25343 variables (22500 binary + 2843 continuous) and 25476 constraints (1576 equality + 23900 inequality) for the 24-node RTS-96 test system.

In contrast to the power system problem, the uncertainty-aware gas pipeline scheduling problem (23) requires 16848 variables and 16512 constraints (16224 equality and 288 inequality) for the single pipe problem.

A. 3-Bus Power System and 1-Pipe Gas System

We simulate uncertainty management for a 3-bus power system with a gas-fired generator at node P1 fueled by a single pipeline gas network, as shown in Fig. 2. The pipe is $L = 30$ km in length with diameter $d = 0.9144$ meters and friction factor $\lambda = 0.05$, and is discretized into shorter segments of 10 km length to create a pipeline graph with 3 edges.

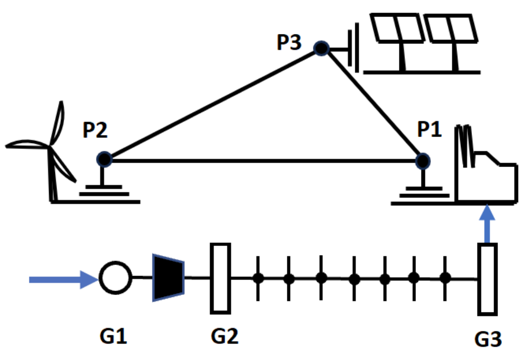

Fig. 2. 3-bus power grid and 1-pipe gas-grid test system

Solving the chance-constrained DC OPF problem with 50 stochastic scenarios requires < 0.01 CPU seconds (CPUs) and yields the power production and reserve schedule shown for power node P1 in Figure 3.

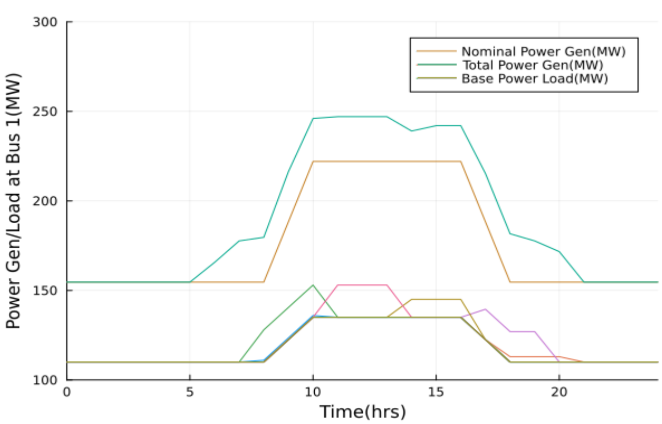

Fig. 3. Power solution at node P1. The base power load and 5 of 50 stochastic load scenarios are shown, in addition to the nominal production schedule and the total (including reserves).

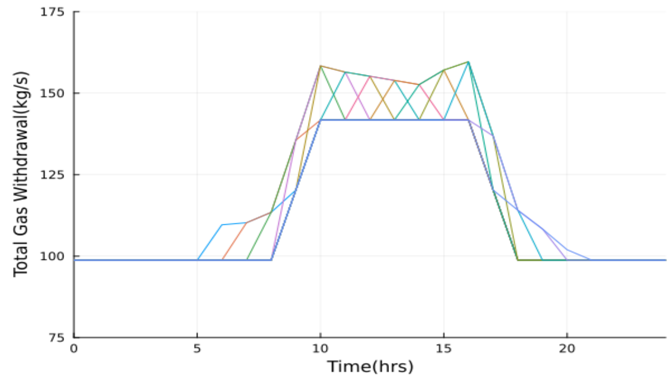

Fig. 4. Stochastic gas demand at node G3. The bottom profile is the baseline consumption, and the sequence of 2-hour consumption increase contingencies, starting at $t_s \in [6, 18]$ hours and weighted according to the reserve schedule, are superimposed above.

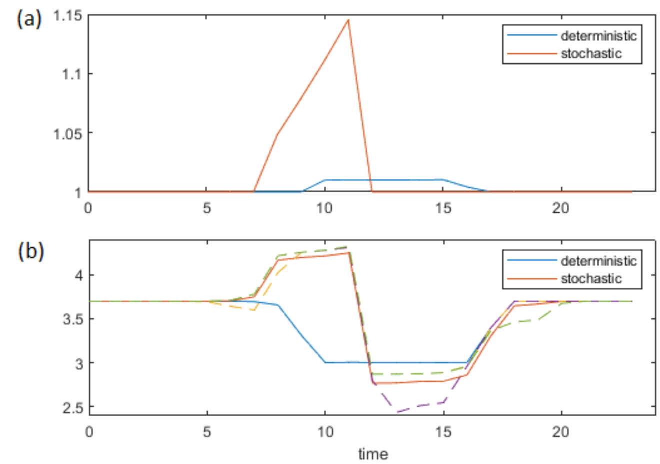

Fig. 5. (a) Solutions for compressor $(1, 2)$ for deterministic and stochastic DOGF. (b) Comparison of solutions for pipeline pressure (MPa) at node G3 for DOGF and average pressure $\mathbb{E}_\omega p_3(t, \omega)$ at node G3 for the stochastic DOGF. Pressure trajectories for three of the stochastic cells corresponding to $t_s \in \{6, 12, 18\}$ are shown as well.

Translating the production and reserve schedules through a heat rate curve with $R_h = 52.2$ MJ/kg and 30% generator efficiency results in stochastic gas consumption at gas node G3 as shown in Figure 4. We now contrast solutions to the deterministic and stochastic DOGF problems in (18) and (23), with hard and probabilistic constraints for the minimum pressure at $p^{\min} = 3$ MPa. The stochastic DOGF problem (23) for one pipe requires 7 CPUs to terminate after warm-start with a deterministic steady-state solution, which requires 0.03 CPUs. Solving the DOGF with no uncertainty requires 0.12 CPUs. We contrast the compressor ratio solutions of the stochastic and deterministic DOGF problems in Fig. 5(a), and examine pressure solutions in Figure 5(b). Observe in Fig. 5(b) that at times of peak demand, the pressure solution in the deterministic case (no scenarios $s \in \mathsf{S}$ occur) binds at the 3MPa minimum. The stochastic solution allows some violation of the constraint, and on average the pressure will be somewhat lower during a part of the optimization horizon. If the deterministic solution were applied and a scenario $s \in \mathsf{S}$ were to occur, the violation would be much more significant.

B. 24-Bus Power System and 24-Pipe Gas System

We applied our stochastic optimal control formulation to the case study constructed with the IEEE RTS-96 24-node power test system coupled to a 24-pipe gas pipeline test network, which is described in detail in previous studies [3], [9]. The chance-constrained OPF for the 24-bus power network in (13) requires 87 CPUs to solve to local optimality. Transforming the power production and reserve allocation schedules to a stochastic gas flow schedule according to (19) leads to a stochastic DOGF problem. Solving the steady-state problem using averaged boundary values results in a problem with 1513 variables and 1492 constraints, which requires only 0.16 CPUs to solve. The deterministic DOGF problem is solved using the same discretization as the stochastic problem, with no uncertainty and thus uniformity across the stochastic space, leading to a NLP with 216888 variables and 123552 constraints that requires 6.65 CPUs to solve. The full stochastic DOGF problem is formulated with 216888 variables and 214272 constraints, and requires 655 CPUs to solve.

V. Conclusions

We described a two-stage optimal control formulation in which a stochastic finite volume representation for nonlinear gas flow with uncertain boundary conditions is used to manage intertemporal uncertainties for a pipeline system that supplies fuel to peaking plants, which provide operating reserves to an electricity market. The concept addresses a key concern in coordination of power systems, gas-fired generation, and gas pipelines indicated by our previous study [9], by ensuring electricity production and probabilistic reserves while maintaining adequate pipeline pressures. Moreover, the formulation calibrates power system production and reserves as well as pipeline flow schedules with probabilistic guarantees using chance constraints for both networks.

The study motivates several challenges to be addressed. While we have demonstrated that stochastic optimal control formulations that can account for intertemporal uncertainty can be formulated and are tractable for general-purpose nonlinear programming solvers, the convergence and accuracy properties, and sensitivity to violation penalty γ and violation probability ϵ_g remain to be characterized. Potential benefits of the approach to increase pipeline capacity by permitting low probability, small amplitude lower pressure constraint violations due to power grid uncertainty may be quantified. This will require defining an economic objective function in expectation and a probabilistic metric for constraint violation, and the comparison of multiple operating scenarios. Finally, the complex evolution of probability distributions of time-dependent pressure and flow trajectories across a network system requires creative concepts for visualizing the optimization solutions.

Acknowledgement

Work at Los Alamos National Laboratory is done under the auspices of the National Nuclear Security Administration under U.S. D.O.E. Contract No. 89233218CNA000001.

References

[1] IEA, "Gas," https://www.iea.org/fuels-and-technologies/gas, 2023, [Online; accessed 27-June-2023].

[2] J. Bistline, "Natural gas, uncertainty, and climate policy in the US electric power sector," *Energy Policy*, vol. 74, pp. 433–442, November 2014.

[3] A. Zlotnik, L. Roald, S. Backhaus, M. Chertkov, and G. Andersson, "Coordinated scheduling for interdependent electric power and natural gas infrastructures," *IEEE Transactions on Power Systems*, vol. 32, no. 1, pp. 600–610, 2016.

[4] C. He, L. Wu, T. Liu, W. Wei, and C. Wang, "Co-optimization scheduling of interdependent power and gas systems with electricity and gas uncertainties," *Energy*, vol. 159, pp. 1003–1015, 2018.

[5] B. Zhao, A. J. Conejo, and R. Sioshansi, "Unit commitment under gas-supply uncertainty and gas-price variability," *IEEE Transactions on Power Systems*, vol. 32, no. 3, pp. 2394–2405, 2016.

[6] S. Chen, A. J. Conejo, and Z. Wei, "Gas-power coordination: from day-ahead scheduling to actual operation," *IEEE Transactions on Power Systems*, vol. 37, no. 2, pp. 1532–1542, 2021.

[7] D. Bienstock, M. Chertkov, and S. Harnett, "Chance-constrained optimal power flow: Risk-aware network control under uncertainty," *Siam Review*, vol. 56, no. 3, pp. 461–495, 2014.

[8] L. Roald and G. Andersson, "Chance-constrained ac optimal power flow: Reformulations and efficient algorithms," *IEEE Transactions on Power Systems*, vol. 33, no. 3, pp. 2906–2918, 2017.

[9] L. A. Roald, K. Sundar, A. Zlotnik, S. Misra, and G. Andersson, "An uncertainty management framework for integrated gas-electric energy systems," *Proceedings of the IEEE*, vol. 108, no. 9, pp. 1518–1540, 2020.

[10] S. Misra, M. Vuffray, and A. Zlotnik, "Monotonicity properties of physical network flows and application to robust optimal allocation," *Proceedings of the IEEE*, vol. 108, no. 9, pp. 1558–1579, 2020.

[11] S. Gerster, M. Herty, M. Chertkov, M. Vuffray, and A. Zlotnik, "Polynomial chaos approach to describe the propagation of uncertainties through gas networks," in *Progress in Industrial Mathematics at ECMI 2018*. Springer, 2019, pp. 59–65.

[12] S. Tokareva, A. Zlotnik, and V. Gyrya, "Stochastic finite volume method for uncertainty quantification of transient flow in gas pipeline networks," *arXiv preprint arXiv:2204.06431*, 2022.

[13] L. Roald, F. Oldewurtel, T. Krause, and G. Andersson, "Analytical reformulation of security constrained optimal power flow with probabilistic constraints," in *2013 IEEE Grenoble Conference*. IEEE, 2013, pp. 1–6.

[14] T. W. Mak, P. V. Hentenryck, A. Zlotnik, and R. Bent, "Dynamic compressor optimization in natural gas pipeline systems," *INFORMS Journal on Computing*, vol. 31, no. 1, pp. 40–65, 2019.

[15] M. Herty, "Modeling, simulation and optimization of gas networks with compressors," *Networks and Heterogeneous Media*, vol. 2, no. 1, pp. 81–97, 2006.

[16] A. Osiadacz, "Simulation of transient gas flows in networks," *International J. Numerical Methods in Fluids*, vol. 4, no. 1, pp. 13–24, 1984.

[17] S. Grundel, L. Jansen, N. Hornung, T. Clees *et al.*, "Model order reduction of differential algebraic equations arising from the simulation of gas transport networks," in *Progress in Differential-Algebraic Equations: Deskriptor 2013*. Springer, 2014, pp. 183–205.

[18] K. Sundar and A. Zlotnik, "State and parameter estimation for natural gas pipeline networks using transient state data," *IEEE Transactions on Control Systems Technology*, vol. 27, no. 5, pp. 2110–2124, 2018.

[19] A. Zlotnik, M. Chertkov, and S. Backhaus, "Optimal control of transient flow in natural gas networks," in *2015 54th IEEE conference on decision and control (CDC)*. IEEE, 2015, pp. 4563–4570.

[20] A. Rudkevich, A. Zlotnik, X. Li, P. Ruiz *et al.*, "Evaluating benefits of rolling horizon model predictive control for intraday scheduling of a natural gas pipeline market," in *52nd Hawaii International Conference on System Sciences*, 2019, pp. 3627–3636.

[21] Q. Huangfu and J. A. J. Hall, "Parallelizing the dual revised simplex method," *Mathematical Programming Computation*, vol. 10, no. 1, pp. 119–142, 2018.

[22] I. Dunning, J. Huchette, and M. Lubin, "Jump: A modeling language for mathematical optimization," *SIAM Review*, vol. 59, no. 2, pp. 295–320, 2017.

[23] R. H. Byrd, J. Nocedal, and R. A. Waltz, *KNITRO: An Integrated Package for Nonlinear Optimization*. Boston: Springer, 2006, pp. 35–59.